Turkish Journal of Earth Sciences

Volume 34
Number 2 *SI-1*

Article 6

2-20-2025

# Characterization of stone materials from the Roman Caracalla Bath in Ancyra

ZEYNEP TANRIVERDİ

ALİ AKIN AKYOL

YUSUF KAĞAN KADIOĞLU



## Recommended Citation

TANRIVERDİ, ZEYNEP; AKYOL, ALİ AKIN; and KADIOĞLU, YUSUF KAĞAN (2025) "Characterization of stone materials from the Roman Caracalla Bath in Ancyra," *Turkish Journal of Earth Sciences*: Vol. 34: No. 2, Article 6. https://doi.org/10.55730/1300-0985.1955
Available at: https://journals.tubitak.gov.tr/earth/vol34/iss2/6

TÜBİTAK

Turkish Journal of Earth Sciences

http://journals.tubitak.gov.tr/earth/

Research Article

Turkish J Earth Sci
(2025) 34: 211-228

doi:10.55730/1300-0985.1955

# Characterization of stone materials from the Roman Caracalla Bath in Ancyra

**Zeynep TANRIVERDİ[1,*], Ali Akın AKYOL[2], Yusuf Kağan KADIOĞLU[3]**

[1]Department of Restoration and Conservation of Cultural Assets, Faculty of Art, Design and Architecture, Fatih Sultan Mehmet Vakıf University, İstanbul, Turkiye

[2]Department of Conservation and Restoration of Cultural Properties, Faculty of Fine Arts, Ankara Hacı Bayram University, Ankara, Turkiye

[3]Department of Geological Engineering, Faculty of Engineering, Ankara University, Ankara, Turkiye

**Received:** 15.06.2024 • **Accepted/Published Online:** 10.12.2024 • **Final Version:** 20.02.2025

**Abstract**: The Roman Caracalla Bath was built during the reign of Roman Emperor Caracalla (circa AD 200). Today it exists only in the form of wall remnants at the foundation level and functions as an open-air museum. It is located on a mound approximately 2.5-m high along Ulus's Çankırı Street in Ankara. This research paper aims to identify the characterization and implications for provenance of the stone materials used in the construction of the bath by using mineralogical, petrographic, and geochemical definitions. The results obtained from the stone materials also provide guidance for restoration and reinforcement of the bath. In this study, the 13 stone and 2 stone tessera materials were examined using petrographic analysis to determine their provenance, along with X-ray fluorescence analysis to identify their chemical composition. The mineralogical composition of each stone shows that the samples can be classified into five subgroups: andesite, limestone, marble, sandstone, and tuff. The andesite was related to Hüseyingazi-Kale and the limestone to the Haymana region, the marble was from Afyon-İscehisar marble quarry (ancient marble quarry), and the sandstone and tuff was related to the village of Memluk Yuva (cetaceous flysch stone). Moreover, the stone tesserae belong to the radiolarite rock group from the village of Elmadağ Irmak. The petrographic results indicate that the stone samples belong to various rock groups, including sedimentary, metamorphic, and volcanic, each reflecting the distinct chemical characteristics of their respective classifications. These findings reveal that the geological formation of the stone materials used at the foundation level of the Roman Caracalla Bath in Ankara corresponds to the surrounding geology of the Ankara region.

**Key words:** Roman baths, stone, provenance, petrographic analysis, X-ray fluorescence

## 1. Introduction

Bathing was a daily practice and way of life in Roman culture. People used the baths for physical and physiological satisfaction, as well as for entertainment. Especially towards the end of the Republican Period (from 509 BC to 27 BC), visiting baths after a light lunch and a rest had become a habitual activity (Yegül, 2010).

Roman baths were a very popular part of Roman life over a long period due to their multifaceted benefits: stimulating the senses and calming the mind, promoting health through light physical exercise, maintaining physical fitness, and providing social and recreational activities such as playing music, reading poetry, and singing, on both a professional and amateur basis (Wheeler, 2004; Yegül, 2010). Moreover, Roman baths served as socially democratic gathering spaces, free from discrimination based on class, gender, wealth, or color (Yegül, 2010). They also served as economic investments, despite their low entrance fees. Additionally, Roman baths were notable for their unique architectural, construction, and functional technologies. Advancements in material technologies enabled the construction of large bath complexes that could accommodate vast numbers of visitors.

In Ankara, a city that has been home to numerous civilizations since ancient times and was highly civilized during the Roman Period, there are several remnants from that era. These include the Roman Temple of Augustus, Roman Theater, Cardo Maximus, the main street of the city of Rome, and the Column Road, although limited numbers of these structures have survived. The Roman (Caracalla) Bath in Ankara, built by the Empire to serve the public, remains one of the city's significant cultural heritage sites (Mutlu, 2012). The bath provides valuable data on the cultural and social life, architecture, and especially the building and material technology of the Roman period. It was the subject of many historical, archaeological,

* Correspondence: ztanriverdi@fsm.edu.tr

and architectural documents, but no studies have been carried out on characterization of the material used in the construction of the bath. In the scientific literature, there are several geological studies on Ankara's stone monuments, but no detailed study has been conducted on the Roman Caracalla Bath in Ankara (Kırca and Erdem, 2005; Gökdemir et al., 2015; Tokmak and Dal, 2020; Deniz and Kadıoğlu, 2022; Deniz Yağcıoğlu and Kadıoğlu, 2023).

Stone materials from historical monuments provide valuable insights. They often reflect the local geology, and the methods used to process them shed light on the historical period, technological developments, the building materials used, and their origins. Detailed petrographic analysis not only aids in identifying the original material sources, but also helps in matching materials from currently available sources for restoration or reconstruction purposes (Columbu et al., 2021).

In recent years, multianalytical methods have been utilized to identify the scientific characteristics of rocks and determine their provenance[1] (Harrell, 1992; Klemm and Klemm, 2001; Koca et al., 2001; Klemm and Klemm, 2008; Barba et al., 2009; Serra et al., 2010; Lazzarini, 2010; Uchida et al., 2010; Çeliktaş et al., 2017; Koralay et al., 2021).

The present research, based on analytical techniques, aimed to investigate the characterization and implications for provenance of the stone materials in the Roman Caracalla Bath. Experts carried out detailed petrographic and geochemical studies. After analysis of the stone materials of the bath, the type and provenance of the stone samples were identified. The findings from the stone materials were also utilized to inform the restoration and strengthening of the bath.

## 2. Historical framework

The existence of baths in ancient Ankara is evidenced by an inscription carved at various locations across the city by twelve Ancyra phylae, five copies of which have survived to the present day. These inscriptions indicate that a bath was constructed under the supervision of Tiberius Julius Justus Junianus, a priest and prominent figure in the city (Bosch, 1967; Mitchell, 1977). Although it is not definitively confirmed that the bath referred to in these inscriptions is the Roman Bath in Ankara, numismatic evidence found during archaeological excavations supports the attribution. Coins recovered from the site suggest that the bath was built under the auspices of the priest during the reign of Emperor Caracalla, between AD 212 and 217 (Bosch, 1967). In addition to archaeological data, engravings and photographs of travelers also serve as important documents regarding the bath. In 1701, Tournefort visited Ankara and in his Ancyra engraving he depicted the walls of the Roman Bath on the hill, next to the Ankara city walls (Tournefort, 1717). In 1813, the traveler Kinneir (Kinneir, 1818) mentioned the ruins of architectural pieces and buildings with walls 30 feet high on a hill overlooking the plain, and it is thought they were the Roman Bath. After some of the bath's walls were blown up with dynamite to build the Ministry of Defense building in 1926, a part of the surviving bath walls could be seen for the last time in De Jerphanion's 1928 photographs (De Jerphanion, 1928) (Kadıoğlu et al., 2011) (Figures 1a and 1b).

The scientific excavation at the baths began in 1931, when architectural remains from the classical period were discovered during the construction of Çankırı Street. The excavations continued in 1937, unearthing finds from the Phrygian, Roman, partly Byzantine, Seljuk, and Ottoman periods. During the excavations carried out in the mound between 1938 and 1941, a large part of the bath complex was unearthed, including the caldarium (hot room), prefenarium (furnace), frigidarium (cold room), piscina (pool), tepidarium (warm room), and palaestra (open courtyard) (Dolunay, 1941, 1948). In 1944, excavations started in the south of the bath with the hypothesis that it might be symmetrical, but symmetrical walls corresponding to the north wing walls were not found. Excavator Akok interpreted this result as indicating the bath being left unfinished for some reason (Akok, 1955; Kadıoğlu et al., 2011). Between 1944 and 1947, excavations continued, guided by finds discovered during the construction of new structures in the surrounding area. The most comprehensive literature data on the bath were recorded in this period (Akok, 1968).

Between 1997 and 2001, the Roman Baths in Ankara were transformed into an open-air museum through display, description, and restoration works carried out by the management of the Anatolian Civilizations Museum.[2] From 2000 to 2006, excavations were conducted to connect the site to the outer wall of Ankara Castle. In 2007, excavations began for the colonnaded road, which was unearthed during the Çankırı Street excavations in the Republican period, located to the east of the Palaestra of the baths.[3] In the following periods, various restoration companies undertook some work, with the most comprehensive work initiated in 2010. Preliminary laboratory analyses on the types, properties, and

[1]Akbulut B (2005). An investigation on utilization Gölbaşı and Çubuk (Ankara) andesites as dimension stones. (in Turkish with an abstract in English). MA, Zonguldak Karaelmas Üniversitesi Fen Bilimleri Enstitüsü, Zonguldak, Türkiye.

[2]Turkish Museums (no date). Ankara Roman Baths and Open Air Museum [online]. https://turkishmuseums.com/Uploads/Museum/File/pdf [accessed 26 June 2024].

[3]Rebublic of Türkiye Ministry of Culture and Tourism (no date). Museums - Ankara Roman Baths and Open Air Museum [online]. https://ankara.ktb.gov.tr/TR-152965/museums.html [accessed 19 May 2024].

a)

b)

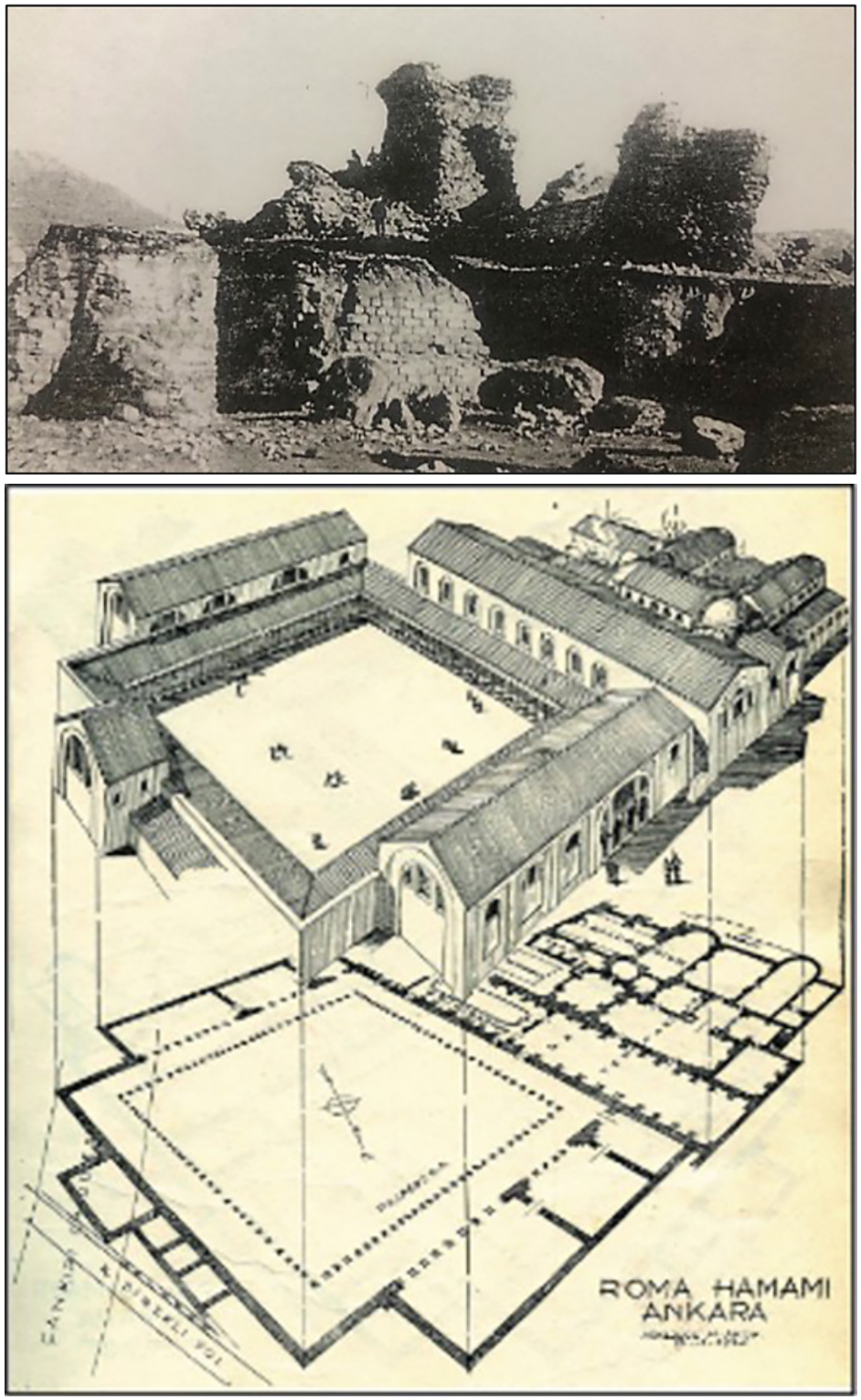


**Figure 1.** (a) Photograph of the last surviving bath walls (De Jerphanion, 1928; Kadıoğlu et al., 2011), (b) The restitution drawing of the Caracalla Bath by Mahmut Akok (Akok, 1968).

deterioration problems of bath building materials were conducted between 2011 and 2014.[4]

In 2013 the Directorate General of Cultural Heritage and Museums designed a tour route for visitors and prepared landscaping projects. The works began in 2014, and wooden walkways and viewing terraces were added around the open-air museum.[5]

In 2022, the Directorate General of Cultural Heritage and Museums initiated restoration and conservation works. As a part of these efforts, the remaining wall joints of the bath were renewed, and capping was applied for their protection. The ancient statues exhibited in the area were placed on platforms to reduce the deterioration caused by the cleared ground, and new walkways and landscaping were added to the bath ruins and palaestra areas.[6]

## 3. Materials and methods

### 3.1. Study area

The Roman (Caracalla) Bath, which consists only of the wall remains at the foundation level, is located on a mound about 2.5-m high on Ulus's Çankırı Street in Ankara. The entrance to the remains, used as an open-air museum, is accessed by stairs from Çankırı Street on the eastern side of the site. Vehicular access to Çankırı Street, which connects the Ulus and Kızılay centers of Ankara and experiences medium traffic density, is provided by a secondary entrance for service vehicles at the northeast corner. To the south of the area there is a high school, to the west commercial units, and to the east car repair shops, hotels, shops, and offices. For security purposes, the entire area is surrounded by stone walls and iron railings 1.10–1.80 m in height, depending on the height difference between the topography and the street (Mutlu, 2012) (Figures 2a and 2b).

The Roman (Caracalla) Bath in Ankara, whose original remains are visible at the foundation level, consists of two parts: the remains of the bath building (blue area on the site plan) and the open area palaestra (red area on the site plan). Based on Akok's studies (1968), who led the excavation, and the on-site examinations, the remains of the bath building include the piscina (P-1) and apodyterium (A-2) in the frigidarium section. These are

[4]Akyol AA. (2012). Ankara Roma (Caracalla) Hamamı Yapı Malzeme Analizi, Raporu, Yayınlanmamış Rapor, Ankara Üniversitesi Yer Bilimleri Uygulama ve Araştırma Merkezi (YEBİM) ve Ankara Üniversitesi Başkent M.Y.O. Malzeme Araştırma ve Koruma Laboratuvarı (MAKLAB) (in Turkish).

[5]General Directorate of Cultural Heritage and Museums (2015). Landscaping Works Begin at Roman Bath in Ankara [online]. https://kvmgm.ktb.gov.tr/TR-131902/ankara-roma-hamami-oren-yerinde-cevre-duzenleme-calismalari-basladi [accessed 09 January 2024].

[6]Daily Sabah (2022). 2000-year-old Roman Baths of Ankara go under restoration [online]. https://www.dailysabah.com/arts/2000-year-old-roman-baths-of-ankara-go-under-restoration/news [accessed 20 July 2024].

a) b)

**Figure 2.** (a) The Google Earth photograph of the Roman (Caracalla) Bath (Google Maps, 2024), (b) The site plan drawing of the Roman (Caracalla) Bath[7], 2024 (updated from Tanrıverdi, 2018).

[7]Nalbant K (2014). Conservation and restoration project reports & drawings of Roman bath in Ankara, Miyar Architectural Office, Ankara, Türkiye.

followed by tepidarium sections (from T-3 to T-14), which form a large part of the bath, the caldarium section (C-15) in the southeast corner, and the water tank (WT-06) (Figure 3).

### 3.2. Sample collection and characterization

Within the scope of the study, a total of 13 stone materials were strategically collected from the foundation level walls of the bath's different temperature sections, including the frigidarium (3 samples), tepidarium (4 samples), and caldarium (5 samples) sections, along with the upper part (1 sample) of the bath. In addition, 3 tessera samples were taken from the piscina (pool) floor of the bath for comparison (Figure 4).

The samples were marked before the analysis in the laboratory. The abbreviations "ARB" for Ankara Roman Bath, "S" for stone, and "Ts" for stone tesserae were used to identify the samples. The samples were first marked on the site plan. Then each sample was photographed with a chart in the laboratory environment (Figure 5). The identification of the samples is presented in Tables 1 and 2.

Laboratory studies, including mineralogical, compositional, and chemical analyses, were carried out at Ankara Hacı Bayram Veli University Historical Materials Research and Conservation Laboratory (MAKLAB) and Ankara University Earth Sciences Application and Research Center (YEBİM) Laboratory.

### 3.3. Analytical techniques

#### 3.3.1. Hardness test (Schmidt hammer)

A hardness test was conducted to assess the strength of the samples in the field. The hardness of the samples was measured using a digital Schmidt hammer, specifically the Digischmidt 2000 from Proceq Testing Instruments. This method was chosen because it is nondestructive and efficient. The hardness of the stones was estimated based on the uniaxial compressive strength of the rocks. The evaluation of the results was carried out by analyzing the rebound values. According to Luke and Snell (2012), the rebound (strength) values for aggregates in concrete are 40 for river rock, 37 for granite, 32 for limestone, and 31 for lightweight aggregates.


**Figure 3.** The remains of the bath building (blue area on the site plan) and the palaestra (red area on the site plan), 2024 (updated from Tanrıverdi, 2018).

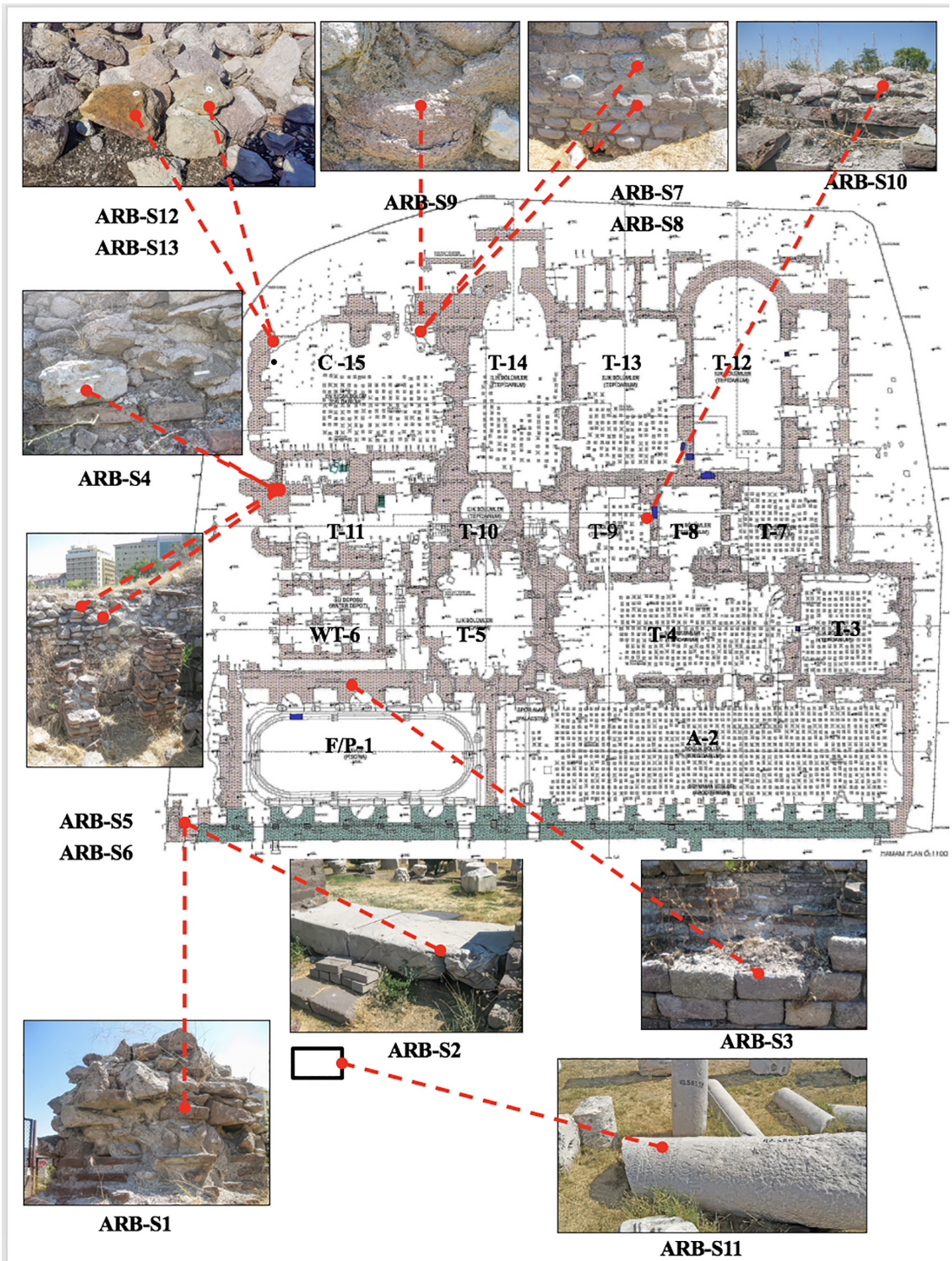


**Figure 4.** Stone sample photographs on the site plan (photos: Tanrıverdi, 2018).

**3.3.2. Petrographic thin section optical microscopy analysis**

Thin section analysis is crucial for identifying the microstructure and mineral compositions of samples collected from the region. Additionally, the analysis can be employed independently to investigate the morphological characteristics of samples (Black et al., 1965; Kerr, 1977; Rapp, 2002; Reedy, 2006). Thin section analysis can also predict the chemical composition of a rock based on its mineralogical formations. To evaluate the mineralogical

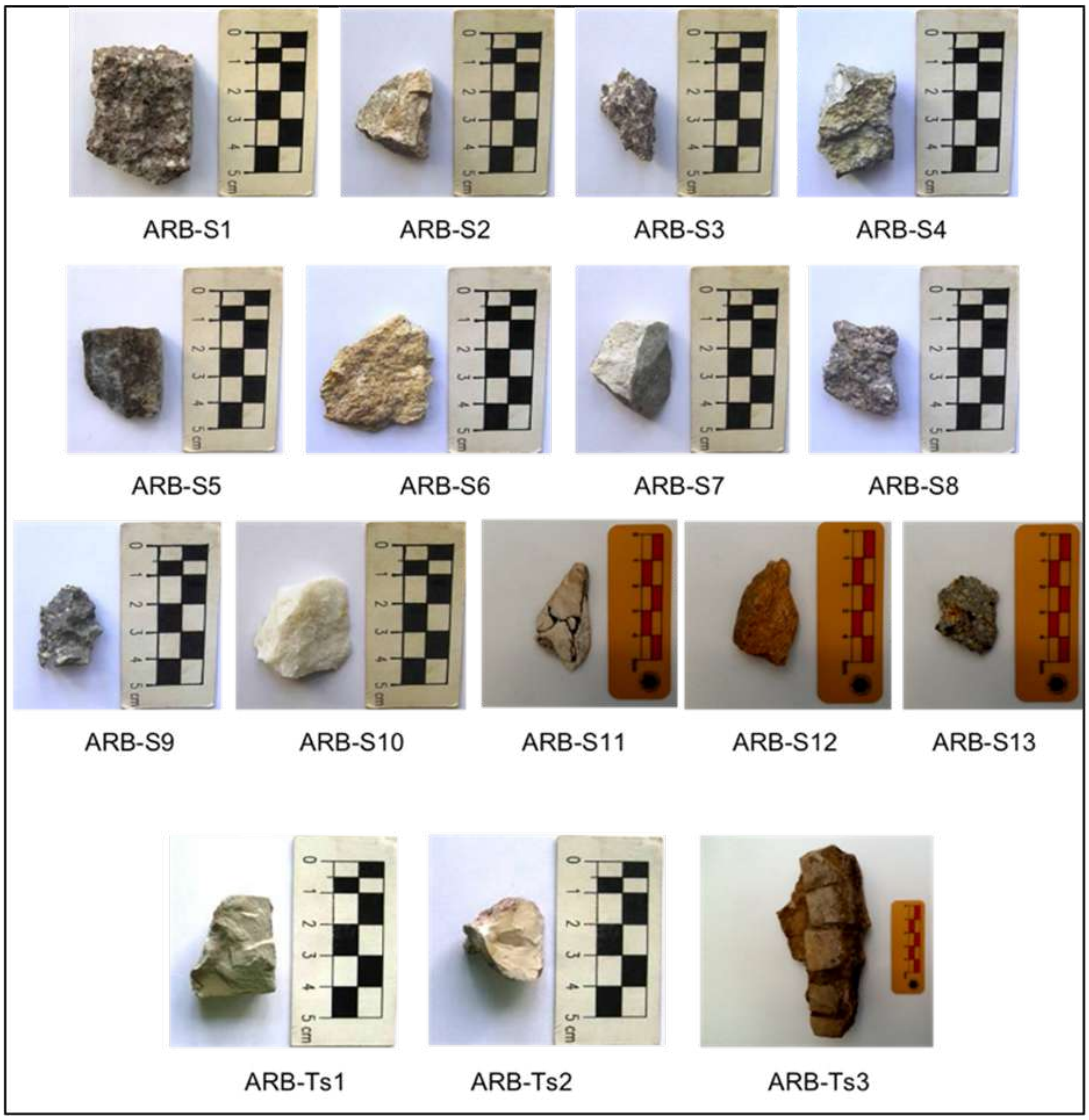


**Figure 5**. Stone sample photographs in the laboratory environment (photos: Tanrıverdi, 2018).

compositions of rocks, several petrochemical calculation methods, such as CIPW, Rittmann, and Niggli, are used to calculate the mineral compositions from the chemical analysis of the samples (Niggli, 1936; Rittmann, 1973; Kadıoğlu, 2001; Wagner, 2022).

In the present study, thin sections were prepared individually from the collected stone samples. Detailed examinations were performed using a Leica DMLP Research Polarizing Microscope equipped with 10, 20, and 100× objectives to determine the mineral composition, textural characteristics, grain shapes, and rock fragment types. Microphotographs of the samples, accompanied by detailed microscopic descriptions, were taken with a Leica DFC 295 color camera attached to the same microscope. The mineral colors in the thin sections were identified using the Michel Levy Interference Color Chart, which is suitable for specimens with a thickness of 0.03 mm (Levy and Lacroix, 1888).

**3.3.3. X-ray fluorescence (XRF) analysis**

XRF analysis involves exposing materials to high-energy X-rays or gamma rays, which excite the atoms in the elements of the material, causing them to emit characteristic "secondary" X-rays. This emission is used to identify the elements present in the material. XRF analysis provides both quantitative and qualitative data on the chemical and elemental characteristics of materials. Qualitative identification focuses on elements with atomic numbers greater than that of oxygen (>8), while quantitative analysis covers all but the lightest elements (Hodges, 1964; Salmon, 1970; Liptak, 2003; Skoog et al., 2007, Shackley, 2011).

**Table 1**. Identification of the collected stone samples.

| Samples | Section | Description |
|---|---|---|
| **ARB-S1** | **F/P-1** | Stone from corner of the southeast stone wall (13) * |
| **ARB-S2** | **F/P-1** | Stone from the base of southeast wall (16) |
| **ARB-S3** | **P-1** | Stone from the west wall of Piscina-1(20) |
| **ARB-S4** | **T-11** | Stone from rubble filled of southwest of Tepidarium-11 (28) |
| **ARB-S5** | **T-11** | Stone from rubble filled of southwest of Tepidarium-11 (29) |
| **ARB-S6** | **T-11** | Stone from rubble filled of southwest of Tepidarium-11 (30) |
| **ARB-S7** | **C-15** | Stone from the northwest wall of Caldarium-15 (41) |
| **ARB-S8** | **C-15** | Highly deteriorated stone from northwest wall of Caldarium-15 (42) |
| **ARB-S9** | **C-15** | Highly deteriorated stone from northwest wall of Caldarium-15 (43) |
| **ARB-S10** | **T-9** | Stone from over the arched of northwest wall of Tepidarium-9 (68) |
| **ARB-S11** | - | Structural component of the upper part (1) |
| **ARB-S12** | **C-15** | Stone from corner of the exterior southwest wall of Caldarium-15 (10) |
| **ARB-S13** | **C-15** | Stone from corner of the exterior southwest wall of Caldarium-15 (11) |

**Table 2**. Identification of the collected stone tessera samples.

| Samples | Section | Description |
|---|---|---|
| **ARB-Ts1** | **P-1** | Stone tessera from base of the niche of the east of Piscina (1)* |
| **ARB-Ts2** | **P-1** | Stone tessera from base of Piscina-1 (9) |
| **ARB-Ts3** | **P-1** | Stone tessera from base of the niche of the east of Piscina-1 (18) |

(*) Specified numbers indicate the order of the sampling

In our study, the major oxide and trace element geochemical analyses of all the samples were conducted using X-Lab2000 Spectro XRF spectrometry. For these analyses, the samples were initially crushed using a Retsch brand jaw crusher, followed by grinding in a tungsten carbide mill with a Fritsch brand grinder. A 4-g portion of the ground sample was mixed with 0.9 g of Wachs (binding material) and compressed under hydraulic pressure to form powder pellets. The analyses were performed using a Spectro X-LAB 2000 Polarized Energy Dispersive Spectrometer, with measurements conducted in a vacuum environment at 15.0 kV and 11.4 mA.

The samples were sieved to pass through 200 μm, and then pressed into thick pellets of 32-mm diameter using a watch as a blinder. USGS standards, GEOL, GBW 7109, and GBW-7309 sediment were equally pressed into pellets in a similar manner as the samples and these used for quality assurance (Timothy and La, 1989; Johnson et al., 1999). The concentrations of the standard samples are given in Table 3.

## 4. Results and discussion

### 4.1. Hardness test (Schmidt hammer) of the stone samples

The hardness test was conducted on only two stones due to the limited amount of samples. The resulting values were utilized to estimate the uniaxial compressive strength of the rock samples. The average rebound (strength) values for ARB-S12 and ARB-S13 were 31.4 and 30.2, respectively (Table 4).

**Table 3**. Concentration of certificated elements in the standard rocks used in the PED-XRF analysis for calibration of the spectrometer and the concentration of standard rocks measured by PED-XRF at a later date to the main analysis.

| Elements | Unit | Certificated concentration G01-MA-N (Granite) | Measured concentration G01-MA-N (Granite) | Certificated concentration K03-MRG-1 (Gabbro) | Measured concentration K03-MRG-1 (Gabbro) |
|---|---|---|---|---|---|
| Na | % | 4.4±0.095 | 4.34 | 0.054±0.5 | 0.044 |
| Mg | % | 0.011±0.0034 | 0.020 | 8.942±0.055 | 8.12 |
| Al | % | 9.026±0.02 | 9.90 | 4.496±0.019 | 5.22 |
| Si | % | 31.48±0.03 | 30.86 | 18.33±0.03 | 18.67 |
| P | % | 0.6676±0.0027 | 0.96 | 0.0371±0.0012 | 0.043 |
| S | ppm | 229.6±2.9 | 232.92 | 779.5±8 | 782 |
| Cl | ppm | 152.3±1.5 | 155.2 | 166±2.2 | 163 |
| K | % | 2.698±0.005 | 2.72 | 0.1558±0.0015 | 0.171 |
| Ca | % | 0.482±0.0018 | 0.54 | 10.33±0.01 | 11.02 |
| Ti | % | 0.00553±0.00006 | 0.0078 | 2.359±0.004 | 2.72 |
| V | ppm | 1.2±0.3 | 1.8 | 668±13 | 662.1 |
| Cr | ppm | 0.7±0.1 | 0.65 | 566.3±3.9 | 569.1 |
| Mn | % | 0.02964±0.00014 | 0.032 | 0.1311±0.0005 | 0.19 |
| Fe | % | 0.339±0.0016 | 0.35 | 12.74±0.01 | 13.10 |
| Co | ppm | 4.0±0.3 | 4.87 | 92.2±6.1 | 94.87 |
| Ni | ppm | 3.4±0.3 | 3.91 | 182.7±3 | 186.21 |
| Cu | ppm | 145.8±0.3 | 149.76 | 129±2 | 131.11 |
| Zn | ppm | 223.9±1.9 | 230.72 | 234.2±2.2 | 235.8 |
| Ga | ppm | 64.9±1.3 | 65.82 | 17.9±0.7 | 16.76 |
| Ge | ppm | 4.6±0.5 | 4.1 | 1±0.4 | 0.65 |
| As | ppm | 13.3±0.6 | 12.72 | 2.4±0.4 | 2.74 |
| Se | ppm | 2.50.4 | 2.82 | 1.4±0.3 | 1.65 |
| Br | ppm | 2.3±0.2 | 2.73 | 0.3±0.2 | 0.20 |
| Rb | ppm | 3648±4 | 3650 | 7.4±0.3 | 7.10 |
| Sr | ppm | 85.1±0.5 | 85.73 | 260.9±0.9 | 269.08 |
| Y | ppm | 0.5±0.1 | 0.8 | 12.5±0.3 | 13.23 |
| Zr | ppm | 27.5±0.3 | 29.9 | 102.7±0.6 | 101.1 |
| Nb | ppm | 171.8±0.5 | 174.2 | 19.5±0.3 | 18.87 |
| Mo | ppm | 1.0±0.2 | 1.2 | 1.5±0.2 | 1.87 |
| Cd | ppm | 2.6±0.3 | 3.0 | 0.5±0.2 | 0.3 |
| Sn | ppm | 861±1.3 | 867.2 | 2.3±0.1 | 2.9 |
| Sb | ppm | 1.6±0.1 | 1.9 | 1±0.2 | 1.5 |
| Te | ppm | 1.5±0.1 | 1.62 | 0.7±0.2 | 1.32 |
| Ba | ppm | 47±1 | 45.2 | 45.6±1 | 47.28 |
| La | ppm | 4.9±0.8 | 5.7 | 8.6±1.3 | 9.27 |
| Ce | ppm | 5.8±0.9 | 6.2 | 26.1±1.7 | 27.9 |
| Pr | ppm | 8.0±1.7 | 8.9 | 8.0±4.7 | 7.1 |
| Nd | ppm | 10±0.9 | 11.2 | 9.5±2.1 | 10.15 |
| Hf | ppm | 5.3±1.4 | 5.87 | 5.9±3.2 | 6.76 |
| Ta | ppm | 290.5±7.1 | 288.6 | 12±0.3 | 11.61 |
| Hg | ppm | 1.6±0.8 | 1.98 | 1.3±0.3 | 0.91 |
| Pb | ppm | 31.6±1.1 | 33.5 | 7.4±0.8 | 6.4 |
| Bi | ppm | 1.3±0.7 | 1.76 | 1.0±0.3 | 1.87 |
| Th | ppm | 1.5±0.2 | 1.66 | 1.5±0.2 | 0.95 |
| U | ppm | 13.2±3.4 | 12.8 | 1.6±0.5 | 1.81 |

**Table 4.** Hardness test results of the stone samples.

| Samples | Mesur. 1 | Mesur. 2 | Mesur. 3 | Mesur. 4 | Mesur. 5 | Average | Type |
|---|---|---|---|---|---|---|---|
| **ARB-S12** | 31.0 | 31.0 | 31.0 | 32.0 | 32.0 | **31.4** | Tuff |
| **ARB-S13** | 29.0 | 30.0 | 30.0 | 31.0 | 31.0 | **30.2** | Andesite |

When these results are compared with those in the study by Luke and Snell (2012), it is evident that ARB-S12 and ARB-S13 fall within the lightweight stone category. Consequently, ARB-S12 has been identified as tuff based on XRF and thin section analyses.

**4.2. Thin section determination of the stone samples**

The thin section determinations were applied to all the samples from the Roman Bath to determine the microstructure, mineral phases, and nature of the stones.

Through this analysis, various layers of the thin section chips were examined under an optical polarized microscope and the findings are discussed as follows.

**4.2.1. Stone samples**

The thin section analysis indicated that the stones can be categorized into five rock subgroups: quartz andesite, limestone (biosparitic, dolomitic, and meta limestone), sandstone, marble, and vitrified tuff. The quartz andesite samples and limestone are further divided into three subgroups, while the sandstone, tuff, and marble samples each belong to a single subgroup.

The andesite has hyalopilitic textures and is composed mainly of oligoclase, andesine, biotite, and amphibole with lesser amounts of opaque minerals. Some of the andesite has amphibole and biotite as mafic minerals and some of the andesites have pyroxene mafic minerals in addition to the amphibole and biotite. Some of the amphibole and biotite are opacified (the secondary formation of the opaque minerals) and the plagioclases are smoothly clay field (the clay formation) on their surfaces under the microscope.

The blasto crystalline texture forms the main textural feature of the meta limestone under the microscope. The limestone has micritic and sparitic texture and is mainly composed of calcite with a minor amount of opaque minerals. All the limestone has an abundant number of fossils and fragments of fossils under the microscope.

The sandstone has a detritic texture with a carbonate matrix and is mainly represented by quartz, plagioclase, biotite, chlorite, epidote, and sericite mineral compositions. Therefore, the bath predominantly features andesite, with later additions of sandstone and limestone, used either as block material or rubble fill in the foundation walls (Figure 6; Table 5).

Additionally, as a part of the geological studies, the origins of all stones were determined. The results indicate that the andesite samples may be from the Hüseyingazi-Kale Formation, limestone samples from the Haymana Formation, sandstone and vitrified tuff samples from the villages of Memluk and Yuva, and the marble samples from the ancient Afyon marble quarry (Kadıoğlu et al., 2018; Deniz Yağcıoğlu and Kadıoğlu, 2023).

**4.2.2. Stone tessera samples**

Thin section analyses were conducted on the stone tesserae and their mortar layers (tessellatum and setting bed) from the mosaics in the piscina. Although ancient mosaics typically have four layers (rudus, nucleus, setting bed, and tessellatum) (Palomar et al., 2011), not all layers are visible in stone tesserae and mortars of the pool. In the examination, only the nucleus and setting bed layers were clearly distinguished (Figure 7). The results indicate that the tessera samples belong to the rock group of radiolarite and originate from the village of Elmadağ Irmak near Ankara (Table 6; Figure 8).

**4.3. XRF analysis of the stone samples**

The results of the XRF analysis provide insights into the chemical compositions of the stone samples. Trace element compositions are particularly crucial for identifying the raw material sources of the samples.

The analyses indicate that stone samples from various rock groups (sedimentary, volcanic, and metamorphic) exhibit chemical characteristics typical of those groups. Andesite samples display consistent ratios for $SiO_2$, averaging 62.91%, and $Al_2O_3$, averaging 12.03% (Table 7a).

The average CaO content, a major oxide in limestone, is 59.99%, whereas in the marble sample (ARB-S10), it is 59.19%. Similarly, the average carbonate content (LOI: loss on ignition), another significant major oxide in limestone, is 37.80%, compared to 39.43% in the marble sample.

In contrast, the major oxide compositions of tuff (ARB-S12) are $SiO_2$, averaging 62.08%, and $Al_2O_3$, averaging 12.27%, while those of sandstone (ARB-S8) are $SiO_2$, averaging 57.16%, and $Al_2O_3$, averaging 11.04% (Table 7b).

The trace elements identified are listed. These results confirm that their chemical compositions are representative of their respective rock groups. Based on the major oxide composition results from the XRF analysis, andesite is categorized into three groups on a triangular plot. Two of these groups indicated largely comparable values, whereas the other group primarily was concentrated on repairing the samples (Figure 9).

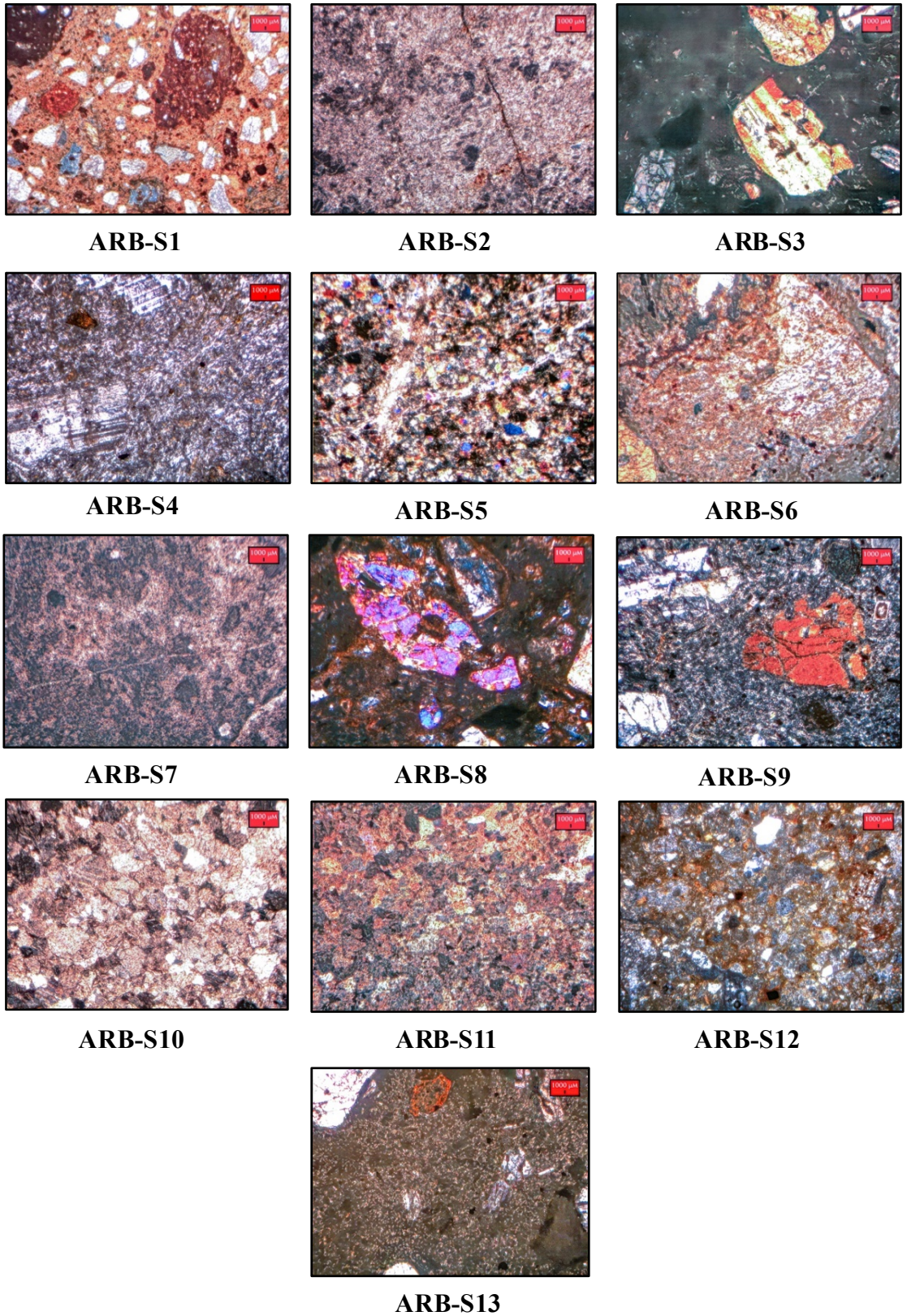


**Figure 6**. Thin section microphotographs of the stone sample (photos: Kadıoğlu, 2024).

**Table 5**. The mineropetrographic properties of the stone samples.

| Stone groups | Rock types | Hardness (Mohs) | Rock and mineral compositions * | Texture | Alterations and deformations |
|---|---|---|---|---|---|
| **Stone Gr1a** (ARB-S1, ARB-S3 ARB-S13) | Quartz Andesite | 6–6.5 | Qzt, Pl,Ad,Amp, Bt,Opq,Mag,Px | Hyalopilitic Porphyric | |
| **Stone Gr1b** (ARB-S5) | Andesite | 6–6.5 | Pl,Amp,Olg | Hyalopilitic Porphyric | Opacified structure |
| **Stone Gr1c** (ARB-S4, ARB-S6 ARB-S9) | Quartz Andesite | 6–6.5 | Qzt,Pl,Amp,Bt,Olg | Hyalopilitic | Opacified and clayey structure |
| **Stone Gr2a** (ARB-S2) | Biosparitic Limestone | 2.5–3 | Cal | Sparitic | Microfractures/cracks filled with recrystallized calcites |
| **Stone Gr2b** (ARB-S7) | Dolomitic Limestone | 2.5–3 | Cal, Dol | Sparitic | Microfractures/cracks filled with recrystallized calcites |
| **Stone Gr2c** (ARB-S11) | Meta Limestone | 2.5–3 | Cal, Qz,Opq,Arg | Micritic Sparitic | |
| **Stone Gr3** (ARB-S8) | Sandstone | 4.5–5 | Qz,Pl,Bt,Chl,Ep,Sr | Detritic | Microfractures/cracks filled with recrystallized calcites, amorphous silicates |
| **Stone Gr4** (ARB-S10) | Marble | ~3 | Cal, Ms,Opq | Granoblastic | Calcite twins with 0.3 mm grain size |
| **Stone Gr5** (ARB-S12) | Tuff | 2–2.5 | Bz,Ad,Qzt,Pl,Bt, Chl,Amp,Sr,Cal,Opq | Hyalopilitic | Opacified biotite and amphiboles |

(*) Ad: Andesite, Amp: Amphibole, Arg: Aragonite, Bz: Basalt, Bt: Biotite, Cal: Calcite, Chl: Chlorite, Dol: Dolomite, Ep: Epidote, Gr: Granite, Mag: Magnetite, Ms: Muscovite, Olg: Oligoclase Andesine, Opq: Opaque Minerals, Pl: Plagioclase, Px: Pyroxene, Qz: Quartz, Qzt: Quartzite, Rd: Radiolarite, S: Sandstone, Sr: Sericite. (The mineral abbreviations are taken from Warr, 2021).

The total LOI values in the geochemical results are more than 11.90%, indicating extremely altered rock units. The results of the major oxide may indicate a clay formation of the plagioclases and opacification of the biotite, amphibole, and pyroxene minerals of the andesite.

## 5. Conclusion

Our research paper seeks to determine the characteristics and provenance of the stone materials used in the construction of the Roman Bath in Ankara through mineralogical, petrographic, and geochemical analyses.

The geology of Ankara covers a variety of rock types and geological formations that have developed over different geological periods. The basement rock units of Ankara are mostly represented by metamorphic and sedimentary rock units. The limestone and claystone formations played a significant role in the development of groundwater resources and the region's geological structure. Most of the volcanic activity started in the Cenozoic period and was mainly characterized by basalt and wide exposure to andesite, significantly influencing the topography of the region. The andesite is mainly named Ankara andesite. All these rock units are covered by soil forming alluvial and sedimentary debris, formed from sediment deposits brought by rivers and rainfall. The geological structure of Ankara is rich in groundwater resources and minerals, which are vital for agriculture and industry. The geology of Ankara plays a crucial role in understanding natural hazards, urban development, and resource management. Geological research and mapping are essential for effective city planning and infrastructure development in the region.

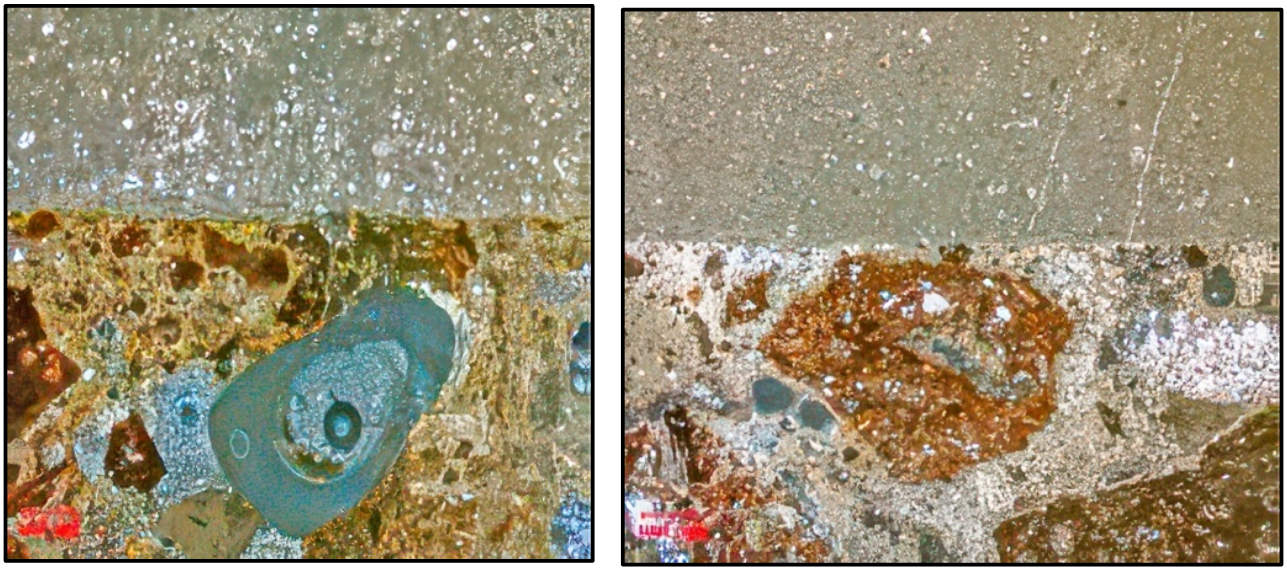


**Figure 7.** Thin section microphotographs of the stone tessera samples (photos: Kadıoğlu, 2024).

**Table 6.** The petrography results of stone tesserae and their mortar layers.

| Stone tessera | Rock types | Hardness (Mohs) | Explanation |
|---|---|---|---|
| **ARB-Ts1 ARB-Ts2** | Radiolarite | 5.5–6 | Radiolarites are formed from epioceanic sediments, which constitute the uppermost layer of the ocean. These radiolarites contain radiolaria fossils and are transported as bed material, often found in mortar. Observations indicate the presence of amorphous silica, small quantities of chalcedony, calcite, and opaque minerals. |
| **Related tessera mortar** | The composition consists of approximately 50% carbonate and marble dust matrix. The remaining 50% is evenly divided, with about 25% comprising aggregate materials (including andesite, limestone, chert, basalt, quartz, plagioclase, and radiolarian fossils) and 25% consisting of brick fragments." | | |

In this context, as a result of petrographic analyses, the stone samples were classified into five groups—andesite, limestone, sandstone, tuff, and marble—in accordance with the geology of Ankara and its immediate surroundings. The geological, petrographic, and geochemical results reveal that the stones of the Roman Caracalla Bath mainly represent the andesite volcanic rocks taken from Hüseyingazi and Yenidoğan andesite rocks. Furthermore, the other main stones of the Roman Bath are limestone and meta limestone taken from the Akyurt and Haymana formation. The sandstone of the Roman Caracalla Bath mainly overlaps more with the features of the Haymana formation's flysch stones. The andesite stones of the Roman Bath are in the compositions of quartz andesite and normal andesite. These features may show that the source of the quartz andesite was Yenidoğan, while the normal andesite originated from Hüseyingazi. The andesite samples were further classified into three subgroups, all sourced from Hüseyingazi Kale. The limestone samples were categorized into three subgroups—biosparitic, dolomitic, and meta limestone—originating from Haymana. The sandstone and tuff samples were grouped into one group together and were sourced from the village of Memluk Yuva. The marble samples were categorized into one group and were sourced from the ancient quarry in Afyon. The stone tessera samples were categorized into the radiolarite rock group, with their formation identified as coming from the Irmak Village Formation of Elmadağ, near Ankara. These results obtained are further supported by isotope studies. Additionally, conducting similar studies on samples

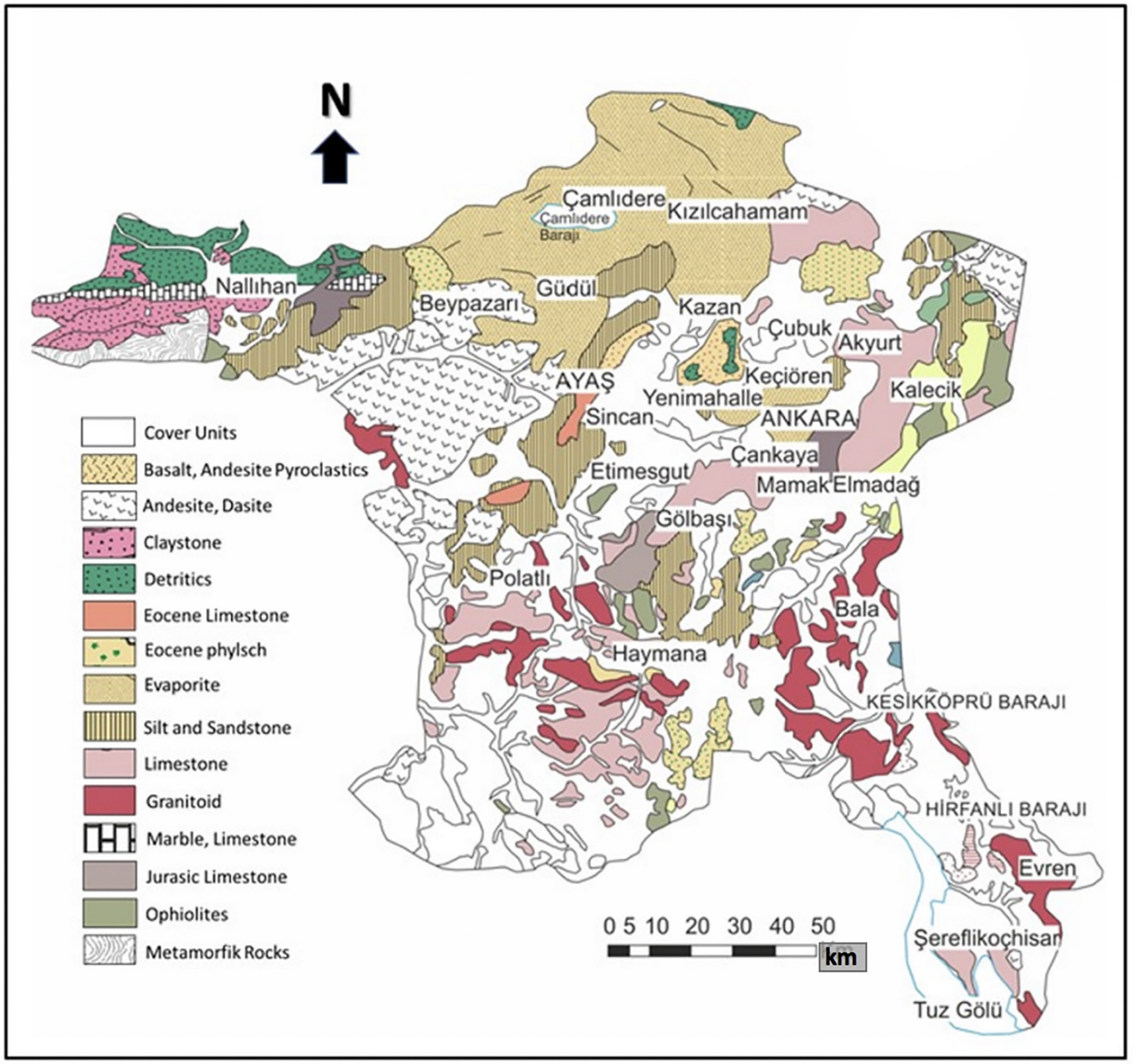


**Figure 8.** Geological map of Ankara (modified from MTA, 2002).[8]

[8]General Directorate of Mineral Research and Exploration (2002). 1:500 Scale Geological Maps of Türkiye [online]. https://www.mta.gov.tr/en/maps/geological-500 [accessed 01 September 2024].

collected from areas identified as source locations would provide stronger validation for the proposed results.

The results of the XRF analysis reveal that the stones exhibit distinct chemical characteristics corresponding to their respective rock groups (sedimentary, metamorphic, volcanic, etc.). The triangle plotting schema indicated that the andesite samples could be categorized into three groups. Two of these groups exhibited mostly similar values; the different one was mostly repairing samples.

All these findings suggest that the geological origin of the stone materials used in the foundation of the Roman Caracalla Bath in Ankara aligns closely with the local geology of the Ankara region.

**Conflict of interest**

The authors declare that they have no known competing financial interests or personal relationships that could have appeared to influence the work reported in this paper.

**Table 7a.** The X-ray fluorescence (PED-XRF) analysis results of andesite stones.

| Element | Dim. | ARB-S1 | ARB-S3 | ARB-S4 | ARB-S5 | ARB-S6 | ARB-S9 | ARB-S13 | Ave. |
|---|---|---|---|---|---|---|---|---|---|
| $Na_2O$ | % | 2.64 | 2.82 | 2.78 | 1.61 | 3.69 | 3.02 | 2.01 | **2.65** |
| MgO | | 1.22 | 1.12 | 0.993 | 2.07 | 0.781 | 0.768 | 1.51 | **1.21** |
| $Al_2O_3$ | | 11.63 | 12.75 | 12.99 | 6.44 | 14.45 | 12.81 | 13.12 | **12.03** |
| $SiO_2$ | | 58.27 | 61.57 | 63.84 | 65.62 | 65.14 | 61.06 | 64.86 | **62.91** |
| $P_2O_5$ | | 0.152 | 0.167 | 0.211 | 0.118 | 0.201 | 0.197 | 0.246 | **0.185** |
| $SO_3$ | | 0.300 | 0.570 | 0.920 | 0.774 | 0.211 | 0.936 | 0.060 | **0.539** |
| Cl | | 0.000 | 0.025 | 0.018 | 0.018 | 0.0002 | 0.028 | 0.0002 | **0.013** |
| $K_2O$ | | 2.24 | 2.81 | 2.84 | 0.430 | 3.51 | 2.76 | 2.27 | **2.41** |
| CaO | | 4.11 | 2.90 | 2.92 | 1.40 | 1.01 | 3.42 | 4.34 | **2.87** |
| $TiO_2$ | | 0.383 | 0.453 | 0.525 | 0.289 | 0.483 | 0.467 | 0.560 | **0.451** |
| $V_2O_5$ | | 0.008 | 0.013 | 0.014 | 0.016 | 0.017 | 0.015 | 0.014 | **0.014** |
| $Cr_2O_3$ | | 0.017 | 0.023 | 0.028 | 0.075 | 0.012 | 0.030 | 0.005 | **0.027** |
| MnO | | 0.058 | 0.018 | 0.019 | 0.107 | 0.017 | 0.018 | 0.073 | **0.044** |
| $Fe_2O_3$ | | 3.08 | 3.23 | 1.80 | 4.86 | 3.05 | 2.40 | 3.66 | **3.15** |
| LOI* | | 16.33 | 11.49 | 10.9 | 16.66 | 7.45 | 12.63 | 7.87 | **11.90** |
| St. types | | **Andesite** | | | | | | | |

**Table 7b.** The X-ray fluorescence (PED-XRF) analysis results of stones.

| Element | Dim. | ARB-S2 | ARB-S7 | ARB-S11 | Ave. | ARB-S8 | ARB-S10 | ARB-S12 |
|---|---|---|---|---|---|---|---|---|
| $Na_2O$ | % | 0.089 | 0.084 | 0.057 | **0.077** | 2.620 | 0.110 | 2.55 |
| MgO | | 0.020 | 0.030 | 0.016 | **0.021** | 1.50 | 0.025 | 0.814 |
| $Al_2O_3$ | | 0.190 | 0.310 | 0.460 | **0.318** | 11.04 | 0.102 | 12.27 |
| $SiO_2$ | | 0.910 | 3.01 | 1.17 | **1.70** | 57.16 | 0.529 | 62.08 |
| $P_2O_5$ | | 0.004 | 0.004 | 0.018 | **0.009** | 0.171 | 0.004 | 0.179 |
| $SO_3$ | | 0.090 | 0.094 | 0.161 | **0.115** | 1.155 | 0.099 | 1.36 |
| Cl | | 0.014 | 0.027 | 0.012 | **0.017** | 0.034 | 0.014 | 0.112 |
| $K_2O$ | | 0.010 | 0.010 | 0.085 | **0.033** | 2.470 | 0.007 | 3.46 |
| CaO | | 60.90 | 58.76 | 60.30 | **59.99** | 5.690 | 59.19 | 2.32 |
| $TiO_2$ | | 0.003 | 0.015 | 0.027 | **0.015** | 0.412 | 0.003 | 0.492 |
| $V_2O_5$ | | 0.002 | 0.002 | 0.001 | **0.002** | 0.016 | 0.002 | 0.016 |
| $Cr_2O_3$ | | 0.004 | 0.009 | 0.002 | **0.005** | 0.042 | 0.003 | 0.008 |
| MnO | | 0.038 | 0.013 | 0.004 | **0.018** | 0.013 | 0.009 | 0.021 |
| $Fe_2O_3$ | | 0.080 | 0.150 | 0.091 | **0.109** | 3.480 | 0.043 | 4.86 |
| LOI* | | 37.83 | 37.83 | 37.75 | **37.80** | 14.34 | 39.43 | 9.85 |
| St. types | | **Limestone** | | | | **Sandstone** | **Marble** | **Tuff** |

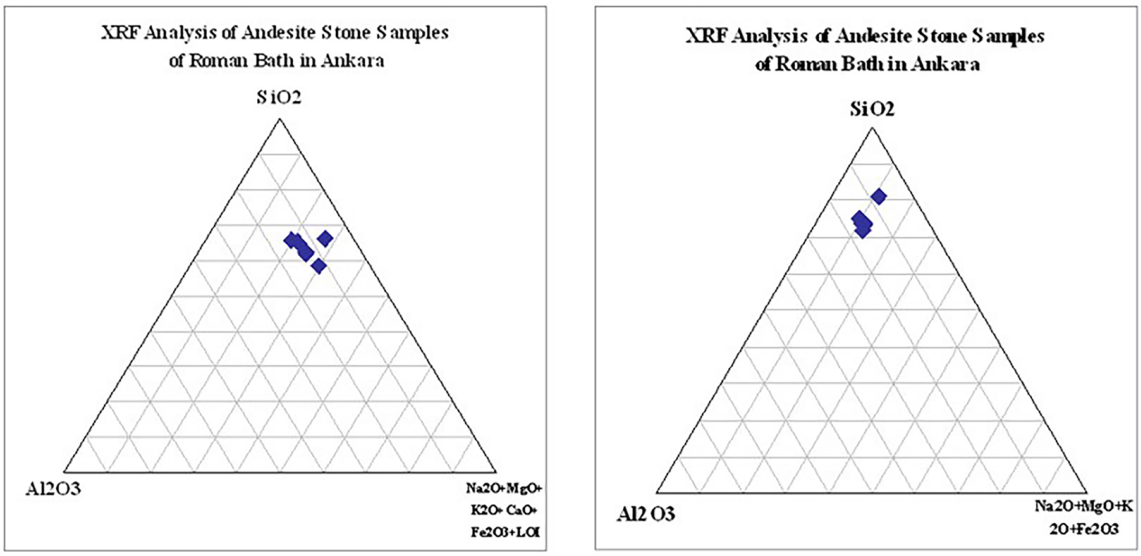


**Figure 9.** XRF analysis triangle plotting of andesite stones: (a) $SiO_2$-$Al_2O_3$-$Na_2O$+MgO+$K_2O$+CaO+$Fe_2O_3$+LOI, (b) $SiO_2$-$Al_2O_3$-$Na_2O$+MgO+$K_2O$+$Fe_2O_3$.

**Acknowledgments**
We would like to thank the Ankara University YEBİM staff and Ankara Hacı Bayram Veli University MAKLAB Laboratory group for analyses of the stone materials.

## References

Akok M (1968). Ankara Şehrindeki Roma Hamamı. Türk Arkeoloji Dergisi 17 (1): 3-37 (in Turkish).

Akok M (1955). Ankara şehri içinde rastlanan ilk çağ yerleşmelerinden bazı izler ve üç araştırma merkezi, Türk Tarih Kurumu. Belleten 19 (75): 309-329 (in Turkish).

Barba L, Blansac J, Manzanilla LR, Ortiz A, Barca D et al. (2009). Provenance of the Limestone Used in Teotihuacan (Mexico): A Methodological Approach. Archaeometry 51 (4): 525-545. https://doi.org/10.1111/j.1475-4754.2008.00430.x

Bosch CE (1967). Quellen zur Geschichte der Stadt Ankara im Altertum, VII / 46, Türk Tarih Kurumu Yayınları, Ankara (in German).

Black CA (1965). Methods of Soil Analysis: (Part 1), Physical and Mineralogical Properties, Including Statistics of Measurements and Sampling. Madison, WI, USA: American Society of Agronomy Inc. https://doi.org/10.2134/agronmonogr9.1

Columbu S, Gaviano E, Costamagna LC, Fancello D (2021). Mineralogical-Petrographic and Physical-Mechanical Features of the Construction Stones in Punic and Roman Temples of Antas (SW Sardinia, Italy): Provenance of the Raw Materials and Conservation State. Minerals 11 (964): 2-34. https://doi.org/10.3390/min11090964

Çeliktaş BG, Kadıoğlu YK, Fener M, Deniz K (2017). Usability of volcanic nature rocks in the vicinity of Ankara volcanics, Türkiye. MERSEM Conference, Antalya, Türkiye, 13-14 December 2017 (in Turkish with an abstract in English).

Dolunay N (1941). Türk Tarih Kurumu Adına Yapılan Çankırıkapı Hafriyatı. Belleten 19 (5): 261-266 (in Turkish).

Dolunay N (1948). Çankırı Kapı Hafriyatı, III. Türk Tarih Kongresi 1943. Türk Tarih Kurumu Yayınları, IX / 3, s. 212-218 (in Turkish).

De Jerphanion G (1928). SJ, Mélanges D'Archaéologie Anatolienne: Monuments Préhelléniques Gréco-Romains, Byzantins et Musulmans de pont, de Cappadoce et de Galatie, Beyrouth Imprimerie Catholique (in French).

Deniz K, Kadıoğlu YK (2022). Origin of Ankara Castle rampart building stones. Ankara Araştırmaları Dergisi 10 (2): 255-271 (in Turkish with an abstract in English). https://dx.doi.org/10.5505/jas.2022.65807

Deniz Yağcıoğlu K, Kadıoğlu YK (2023). Comparison of Building Stones of Ankara Republican Period Buildings with Ankara Castle Building Stones. 43rd International Excavation, Research and Archaeometry Symposium. Ankara, Türkiye, 16-20 October 2023.

Gökdemir A, Demirel C, Yeğin Y, Şimşek Z (2015). Ankara Temple (Monumentum Ancyranum/Temple of Augustus and Rome). Case Studies in Construction Materials 2 (2015): 55-65. https://doi.org/10.1016/j.cscm.2015.02.002

Harrell JA (1992). Ancient Egyptian limestone quarries: a petrological survey. Archaeometry 34 (2): 195-211. https://doi.org/10.1111/j.1475-4754.1992.tb00492.x

Hodges H (1964). Artifacts: An Introduction to Primitive Technology. New York, NY, USA: Praeger Press.

Kadıoğlu YK (2001). Mafik ve Ultramafik Magmatik Kayaçların Ana-Eser REE Jeokimyasal Karakteristikleri ve Jeofiziksel Açıdan İncelenmeleri, Magmatik Petrojenez Lisans Üstü Yaz Okulu, Akçakoca-Düzce, Türkiye. TMMOB Yayınları (61):159-195 (in Turkish).

Kadıoğlu M, Görkay K, Mitchell S (2011). Roman Ancyra. İstanbul, Türkiye: Yapı Kredi Yayınları.

Kadıoğlu SK, Kadıoğlu YK, Akyol AA (2018). Ankara Roma Hamamı'nda Jeofizik ve Petrografik Çalışmalar, 39. Uluslararası Kazı, Araştırma ve Arkeometri Sempozumu, Bursa, Türkiye, 22-26 Mayıs 2017 (in Turkish).

Kerr PF (1977). Optical Mineralogy. New York, NY, USA: McGraw-Hill Book Company.

Kırca Ö, Erdem TK (2005). An experimental study on the construction materials of the Ankara Citadel, IVth International Seminar on Structural Analysis of Historical Constructions, Padua, Italy, 10-13 November 2004.

Kinneir JM (1818). Journey through Asia Minor, Armenia and Koordistan, in the years 1813 and 1814; with remarks of the Marches of Alexander and retreat of the Ten Thousand. London, UK: John Murray Publisher.

Koralay T, Deniz K, Duman B, Kadıoğlu YK (2021). Mineralogical and geochemical characterization and implications for provenance of Roman granite columns in ancient Tripolis (Denizli, Türkiye). Arabian Journal of Geosciences 14 (6): 420. https://doi.org/10.1007/s12517-021-06744-w

Klemm DD, Klemm R (2001). The building stones of ancient Egypt – a gift of its geology. Journal of African Earth Science 33 (3-4): 631-642. https://doi.org/10.1016/S0899-5362(01)00085-9

Klemm R, Klemm DD (2008). Stones and quarries in ancient Egypt. London, UK: British Museum Press.

Koca MY, Yavuz AD, Kıncal C (2001). The usage of andesitic rocks as a coating purpose in Bergama (İzmir) (in Turkish with an abstract in English). MERSEM Conference, Afyon, Türkiye, 3-5 May 2001.

Lazzarini L (2010). Six colored types of stone from Asia Minor used by the Romans, and their specific deterioration problems. Studies in Conservation 55 (2): 140-146. https://doi.org/10.1179/sic.2010.55.Supplement-2.140

Levy AM, Lacroix A (1888). Les Mineraux Des Roches, Librarie Polytechnique, Baudry Et C., Editeurs, Paris (in French).

Liptak BG (2003). Elemental Monitors, Instrument Engineers' Handbook, Process Measurement and Analysis (4th ed., Vol. 1, pp. 1344-1346). Boca Raton, FL, USA: CRC Press.

Luke M, Snell PE (2012). Using the rebound hammer, Senior Materials Engineer, Western Technologies Inc., Poenix AZ, Proceedings of the 11th Annual Mongolian Concrete Conference.

Mitchell S (1977). R.E.C.A.M. Notes and Studies No.1: Inscription of Ancyra, Anatolian Studies (27): 63-103. https://doi.org/10.2307/3642654

Mutlu Ö (2012). Integration of the Roman remains in Ulus Ankara within in the current urban contex. MA, Middle East Technical University, Ankara, Türkiye.

Niggli P (1936). Über Molekularnormen zur Geteinsberechung. Schweizerische Mineralogische und Pettrographische Mitteilungen (16): 295-317 (in German).

Palomar T, García-Heras M, Saiz-Jiménez C, Márquez C, Villegas, MA (2011). Pathologies and analytical study of mosaic materials from Carmona and Italica. Materiales de Construcción 61 (304): 629-636. https://doi.org/10.3989/mc.2011.64310

Rapp G (2002). Archaeomineralogy (Natural Science in Archaeology). New York, NY, USA: Springer.

Reedy CL (2006). Review of digital image analysis of petrographic thin section in conservation research. Journal of the American Institute for Conservation 45 (2): 127-146. https://doi.org/10.1179/019713606806112531

Rittmann A (1973). Stable Mineral Assemblages of Igneous Rocks. New York, NY, USA: Springer.

Salmon ME (1970). An X-ray fluorescence method for micro-samples, IIC American Group Technical Papers from 1968 through 1970. IIC-American Group, New York, pp. 31-46.

Serra M, Borghi A, D'Amicone E, Fiora L, Mashali O et al. (2010). Black and red granites in the Egyptian antiquity museum of Turin, a minero-petrographic and provenance study. Archaeometry 52 (6): 962-986. https://doi.org/10.1111/j.1475-4754.2010.00522.x

Shackley MS (2011). An introduction to X-Ray fluorescence (XRF) analysis in archaeology. In: Shackley M (editor). X-Ray Fluorescence Spectrometry (XRF) in Geoarchaeology. New York, NY, USA: Springer, pp. 7-44. https://doi.org/10.1007/978-1-4419-6886-9_2

Skoog DA, Holler FJ, Crouch SR (2007). Principles of Instrumental Analysis. 6th ed. Belmont, CA, USA: Thomson Brooks/Cole.

Tanrıverdi Z (2018). Archaeometric investigation of the construction materials of Roman (Caracalla) bath in Ankara, PhD, Middle East Technical University, Ankara, Türkiye.

Tokmak M, Dal M (2020). Classification of physical, chemical and biological deteriorations observed in Ankara stone monuments. International Journal of Pure and Applied Sciences 6 (1): 8-16. https://doi.org/10.29132/ijpas.718466.

Tournefort JP (1717). Relation d'un voyage du Levant 3. Lyon (in French).

Uchida E, Ito K, Shimizu N (2010). Provenance of the sandstone used in the construction of the Khmer Monuments in Thailand. Archaeometry 52 (4): 550-574. https://doi.org/10.1111/j.1475-4754.2009.00505.x

Wagner WH (2022). Normative mineralogy especially for shales, slates, and phyllties. In: René M (editor). Mineralogy. London, UK: IntechOpen.

Warr LN (2021). IMA-CNMNC approved mineral symbols. Mineralogical Magazine 85 (3): 291-320. https://doi.org/10.1180/mgm.2021.43

Wheeler M (2004). Roma Sanatı ve Mimarlığı. İstanbul, Türkiye: Homer Kitabevi (in Turkish).

Yegül FK (2010). Roma Dünyasında Yıkanma. İstanbul, Türkiye: Koç Üniversitesi Yayınları (in Turkish).